2008

Computer simulation of architectural and molecular weight effects on the assembly of amphiphilic linear-dendritic block copolymers in solution

Nicholas W. Suek
Iowa State University

Monica H. Lamm
Iowa State University, mhlamm@iastate.edu

Computer simulation of architectural and molecular weight effects on the assembly of amphiphilic linear-dendritic block copolymers in solution

Abstract

Langevin dynamics simulations are performed on linear-dendritic diblock copolymers containing bead-spring, freely jointed chains composed of hydrophobic linear monomers and hydrophilic dendritic monomers. The critical micelle concentration (CMC), micelle size distribution, and shape are examined as a function of dendron generation and architecture. For diblock copolymers with a linear block of fixed length, it is found that the CMC increases with increasing dendron generation. This trend qualitatively agrees with experiments on linear-dendritic diblock and triblock copolymers with hydrophilic dendritic blocks and hydrophobic linear blocks. The flexibility of the dendritic block is altered by varying the number of spacer monomers between branch points in the dendron. When comparing linear-dendritic diblock copolymers with similar molecular weights, it is shown that increasing the number of spacer monomers in the dendron lowers the CMC due to an increase in flexibility of the dendritic block. Analysis on the micellar structure shows that linear-dendritic diblock copolymers pack more densely than what would be expected for a linear-linear diblock copolymer of the same molecular weight.

Keywords

critical micelle concentration (CMC), hydrophilic dendritic monomers, dendrimers, heavy ions, hydrophilicity, micelles block copolymers, polymer

Disciplines

Biochemical and Biomolecular Engineering | Chemical Engineering | Polymer Science

Computer Simulation of Architectural and Molecular Weight Effects on the Assembly of Amphiphilic Linear−Dendritic Block Copolymers in Solution

Nicholas W. Suek and Monica H. Lamm*

Department of Chemical and Biological Engineering, Iowa State University, Ames, Iowa 50011

Received September 28, 2007. In Final Form: December 20, 2007

Langevin dynamics simulations are performed on linear−dendritic diblock copolymers containing bead-spring, freely jointed chains composed of hydrophobic linear monomers and hydrophilic dendritic monomers. The critical micelle concentration (CMC), micelle size distribution, and shape are examined as a function of dendron generation and architecture. For diblock copolymers with a linear block of fixed length, it is found that the CMC increases with increasing dendron generation. This trend qualitatively agrees with experiments on linear-dendritic diblock and triblock copolymers with hydrophilic dendritic blocks and hydrophobic linear blocks. The flexibility of the dendritic block is altered by varying the number of spacer monomers between branch points in the dendron. When comparing linear−dendritic diblock copolymers with similar molecular weights, it is shown that increasing the number of spacer monomers in the dendron lowers the CMC due to an increase in flexibility of the dendritic block. Analysis on the micellar structure shows that linear-dendritic diblock copolymers pack more densely than what would be expected for a linear−linear diblock copolymer of the same molecular weight.

1. Introduction

Amphiphilic linear−dendritic block copolymers have generated interest for their potential use as drug and gene delivery devices because of their ability to form micelles with critical micelle concentration (CMC) values well below the CMC values of traditional surfactants.[1] An additional attractive feature of linear−dendritic block copolymers is that they can be synthesized with low polydispersity and well-defined molecular architecture.[2−5] Linear−dendritic block copolymers have been synthesized with a variety of topologies, including diblock,[3,4,6−11] triblock,[1,2,5,6,12−14] linear comb−dendritic,[15,16] coil−dendron rod,[17,18] and end-grafted dendritic,[19,20] as illustrated in Figure 1. Vesicles, bilayer nanotubes, and spherical and cylindrical micelles, are among the aggregate morphologies that linear−dendritic block copolymers are known to form. Variations in dendron generation and solution pH have been shown to affect the CMC and the aggregate morphology and size;[3−5,21] in some instances, the micellization behavior is unexpected compared to what would be observed for traditional amphiphiles.[3,5] This prompts the need for a better theoretical understanding of the solution-phase behavior of linear−dendritic block copolymers.

There have been relatively few theory or simulation attempts to explain the interesting properties displayed by linear−dendritic block copolymers. The melt state behavior of linear−dendritic block copolymers has been studied theoretically[22,23] and with computer simulation.[24] We are aware of only one previous molecular simulation study directed toward the solution properties of linear−dendritic copolymers. Jang and co-workers used molecular dynamics simulation to conduct a detailed, exploratory analysis of dendron-grafted copolymers as building blocks for improved fuel cell membranes.[25,26] The present study is aimed at systematically exploring the micellization properties of linear−dendritic diblock copolymers, where the dendritic block is hydrophilic and the linear block is hydrophobic. This class of linear−dendritic block copolymer is of special importance for targeted delivery applications where the many end groups of the hydrophilic dendron are expected to reside near the micelle periphery and, thus, can be functionalized with ligands to target cell receptors.

The CMC of traditional surfactant or amphiphilic block copolymer systems varies with the head-to-tail molecular weight ratio (surfactants) or the hydrophilic-to-hydrophobic block

* To whom correspondence should be addressed. E-mail: mhlamm@iastate.edu.

(1) Gitsov, I.; Lambrych, K. R.; Remnant, V. A.; Pracitto, R. *J. Polym. Sci., Part A* **2000**, *38*, 2711−2727.
(2) Gitsov, I.; Wooley, K. L.; Frechet, J. M. J. *Angew. Chem., Int. Ed. Engl.* **1992**, *31*, 1200−1202.
(3) van Hest, J. C. M.; Delnoye, D. A. P.; Baars, M. W. P. L.; van Genderen, M. H. P.; Meijer, E. W. *Science* **1995**, *268*, 1592−1595.
(4) Gillies, E. R.; Jonsson, T. B.; Frechet, J. M. J. *J. Am. Chem. Soc.* **2004**, *126*, 11936−11943.
(5) Nguyen, P. M.; Hammond, P. T. *Langmuir* **2006**, *22*, 7825−7832.
(6) Gitsov, I.; Frechet, J. M. J. *Macromolecules* **1993**, *26*, 6536−6546.
(7) Iyer, J.; Fleming, K.; Hammond, P. T. *Macromolecules* **1998**, *31*, 8757−8765.
(8) Zhu, L. Y.; Zhu, G. L.; Li, M. Z.; Wang, E. J.; Zhu, R. P.; Qi, X. *Eur. Polym. J.* **2002**, *38*, 2503−2506.
(9) Klok, H.-A.; Hwang, J. L.; Hartgerink, J. D.; Stupp, S. I. *Macromolecules* **2002**, *25*, 6101−6111.
(10) Istratov, V.; Kautz, H.; Kim, Y. K.; Schubert, R.; Frey, H. *Tetrahedron* **2003**, *59*, 4017−4024.
(11) Wood, K. C.; Little, S. R.; Langer, R.; Hammond, P. T. *Angew. Chem., Int. Ed.* **2005**, *44*, 6704−6708.
(12) Gitsov, I.; Frechet, J. M. J. *Macromolecules* **1994**, *27*, 7309−7315.
(13) Namazi, H.; Adeli, M. *Eur. Polym. J.* **2003**, *39*, 1491−1500.
(14) Adeli, M.; Zarnegar, Z.; Dadkhah, A.; Hossieni, R.; Salimi, F.; Kanani, A. *J. Appl. Polym. Sci.* **2007**, *104*, 267−272.
(15) Tian, L.; Nguyen, P.; Hammond, P. T. *Chem. Commun.* **2006**, 3489−3491.
(16) Tian, L.; Hammond, P. T. *Chem. Mater.* **2006**, *18*, 3976−3984.
(17) Cheng, C. X.; Huang, Y.; Tang, R. P.; Chen, E. Q.; Xi, F. *Macromolecules* **2005**, *38*, 3044−3047.
(18) Santini, C. M. B.; Hatton, T. A.; Hammond, P. T. *Langmuir* **2006**, *22*, 7487−7498.
(19) Chang, Y.; Park, C.; Kim, K. T.; Kim, C. *Langmuir* **2005**, *21*, 4334−4339.
(20) Park, C.; Lee, I. H.; Lee, S.; Song, Y.; Rhue, M.; Kim, C. *Proc. Natl. Acad. Sci. U.S.A.* **2006**, *103*, 1199−1203.
(21) van Hest, J. C. M.; Baars, M. W. P. L.; Elissen-Roman, C.; van Genderen, M. H. P.; Meijer, E. W. *Macromolecules* **1995**, *28*, 6689−6691.
(22) Pickett, G. T. *Macromolecules* **2002**, *35*, 1896−1904.
(23) Grason, G. M.; DiDonna, B. A.; Kamien, R. D. *Phys. Rev. Lett.* **2003**, 91.
(24) Liu, D. H.; Zhong, C. L. *Macromol. Rapid Commun.* **2005**, *26*, 1960−1964.
(25) Jang, S. S.; Lin, S.-T.; Cagin, T.; Molinero, V.; Goddard, W. A., III. *J. Phys. Chem. B* **2005**, *109*, 10154−10167.
(26) Jang, S. S.; Goddard, W. A. *J. Phys. Chem. C* **2007**, *111*, 2759−2769.

10.1021/la703006w CCC: $40.75
Published on Web 02/21/2008

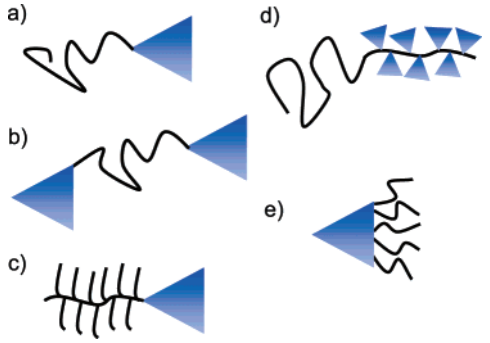

Figure 1. Schematic of representative linear-dendritic block copolymer topologies: (a) diblock, (b) triblock, (c) linear comb−dendritic, (d) coil−dendron rod, and (e) end-grafted dendritic.

molecular weight ratio (block copolymers). Similarly, in linear−dendritic block copolymers the balance between soluble and insoluble entities is tuned by the molecular weight ratio between the dendritic and linear blocks, where the dendritic block molecular weight is altered by varying its generation (i.e., the number of branching points from the dendron core). Experiments on linear−dendritic block copolymers with hydrophobic linear blocks and hydrophilic dendritic or hyperbranched blocks have shown that the CMC increases as the generation of the hydrophilic block increases.[5,10]

The architecture of traditional surfactant chains has also been shown to affect CMC. Recently, Firetto and co-workers[27] performed a systematic study on the effect of chain stiffness on micelle formation with Monte Carlo simulation. In this work the stiffness of the entire chain, the hydrophilic block, and the hydrophobic block were varied separately. The CMC was found to decrease with increasing chain stiffness, with hydrophobic block stiffness having a larger effect on the CMC decrease than hydrophilic block stiffness. The aggregation number, or number of surfactants in the micelle, was shown to increase with increasing hydrophilic group stiffness, in agreement with experimental data comparing hydrogenated and perfluorinated surfactants.[27] The effect of stiffness on the micellization behavior of linear−dendritic block copolymers was studied in refs 5 and 10 by varying the solution pH such that the branches of the dendritic block became stiffer (due to electrostatic repulsions from protonation) as the pH was lowered. In both studies the CMC was observed to increase as the hydrophilic dendritic block became stiffer.

In addition to Monte Carlo, Langevin dynamics has also been successfully used to simulate self-assembly phenomena. Lin et al.[28] investigated the micelle structure of rod−coil diblock copolymers. By changing the segregation strength of rod pairs, they observed structure transitions that agree with previous experiments and theoretical predictions. Langevin dynamics has also been used to study the phase behavior of polymer-tethered nanoparticles,[29−31] the effect of head group size on the micellization of surfactants,[32,33] and the self-assembly of peptides.[34,35]

The aim of this study is to provide fundamental insight about how changes in molecular weight and architecture of the hydrophilic dendritic block in a linear−dendritic block copolymer impact micellization properties. In this paper, we describe Langevin dynamics simulations on linear−dendritic diblock copolymer systems containing bead-spring, freely jointed chains composed of hydrophobic linear monomers and hydrophilic dendritic monomers. We first simulate copolymers with a linear chain length of 30 monomers and dendrons of generation G = 2, 3, 4, and 5, with fixed spacer lengths between branch points D = 1, 2, and 4, to determine the relationship between CMC and dendron generation for a given spacer length. We then compare results for dendrons with different spacer lengths but the same molecular weight to determine the relationship between CMC and dendritic architecture. Finally, we perform simulations on linear−dendritic systems at concentrations above the CMC to examine the effect that variations in dendron generation and architecture have on the micelle size distribution and micelle shape.

2. Method

We simulate the self-assembly of linear dendritic copolymers in an implicit solvent using Langevin dynamics because the solvent occupies more than 80% of the simulation volume in the most concentrated systems we examine. The use of implicit solvent reduces the number of degrees of freedom and is an appropriate simplification because the time scale of solvent molecule motion is shorter than that of a monomer. A heat bath applies a random force and viscous drag to account for uncorrelated solvent contributions. The copolymer chain model consists of bead-spring, freely jointed monomers. The equation of motion for each monomer i of mass m is[36,37]

$$m\ddot{\mathbf{r}}_i(t) = -\nabla \sum_j [U_{\mathrm{LJ}}(r_{ij}) + U_{\mathrm{Bond}}(r_{ij})] - m\xi\dot{\mathbf{r}}_i(t) + \mathbf{W}_i(t) \quad (1)$$

where r_{ij} is the distance between monomers i and j, $\mathbf{r}$ is the position of monomer i, and ξ is the friction coefficient coupling the monomers to the heat bath. The random force, $\mathbf{W}_i$, is Gaussian with zero mean and satisfies,

$$\langle \mathrm{W}_i(t)\cdot\mathrm{W}_j(t')\rangle = 6k_{\mathrm{B}}Tm\xi\delta_{ij}\delta(t-t') \quad (2)$$

where k_{B} is the Boltzmann constant, and T is the temperature. Monomer−monomer interactions, U_{LJ}, are calculated with a truncated and shifted Lennard−Jones interaction potential,[36]

$$U_{\mathrm{LJ}}(r_{ij}) = \begin{cases} 4\epsilon\left[\left(\frac{\sigma}{r_{ij}}\right)^{12} - \left(\frac{\sigma}{r_{ij}}\right)^{6} - \left(\frac{\sigma}{r_{cij}}\right)^{12} + \left(\frac{\sigma}{r_{cij}}\right)^{6}\right], & r_{ij} \le r_{cij} \\ 0, & r_{ij} > r_{cij} \end{cases} \quad (3)$$

where ϵ is the well-depth, σ is the particle diameter, and r_{cij} is the cutoff radius. For all monomers, $\epsilon = 1$, $\sigma = 1$, $m = 1$, and $\xi = 0.5\tau^{-1}$, where $\tau = \sigma\sqrt{m/\epsilon}$. Values selected for the cutoff radius will be discussed below. The bonded monomer attraction, U_{Bond}, is calculated with a finitely extensible nonlinear elastic potential,

$$U_{\mathrm{Bond}}(r_{ij}) = \begin{cases} -0.5kR_0^2 \ln[1 - (r_{ij}/R_0)^2], & r_{ij} \le R_0 \\ \infty, & r_{ij} > R_0 \end{cases} \quad (4)$$

where $k = 25T\epsilon/\sigma^2$ and $R_0 = 1.5\sigma$. These parameters prevent chain crossing by ensuring an average bond length of 0.97σ.[38]

The copolymer molecules are of type $A_{N_d}B_{30}$, where A represents hydrophilic dendritic monomers and B represents hydrophobic linear polymer monomers. The number of monomers, N_d, in the dendritic block is calculated from,

(27) Firetto, V.; Floriano, M. A.; Panagiotopoulos, A. Z. *Langmuir* **2006**, *22*, 6514−6522.
(28) Lin, S.; Numasawa, N.; Nose, T.; Lin, J. *Macromolecules* **2007**, *40*, 1684−1692.
(29) Horsch, M. A.; Zhang, Z.; Glotzer, S. C. *Phys. Rev. Lett.* **2005**, *95*, 056105.
(30) Iacovella, C. R.; Horsch, M. A.; Zhang, Z.; Glotzer, S. C. *Langmuir* **2005**, *21*, 9488−9494.
(31) Zhang, Z.; Horsch, M. A.; Lamm, M. H.; Glotzer, S. C. *Nano Lett.* **2003**, *3*, 1341−1346.
(32) Bourov, G. K.; Bhattacharya, A. *J. Chem. Phys.* **2003**, *119*, 9219−9225.
(33) Bourov, G. K.; Bhattacharya, A. *J. Chem. Phys.* **2005**, *122*, 044702.
(34) Lenoci, L.; Camp, P. *J. Am. Chem. Soc.* **2006**, *128*, 10111−10117.
(35) Bellesia, G.; Shea, J.-E. *J. Chem. Phys.* **2007**, *126*, 245104.
(36) Allen, M. P.; Tildesley, D. J. *Computer Simulation of Liquids;* Clarendon Press: Oxford, 1987.
(37) Grest, G. S.; Kremer, K. *Phys. Rev. A* **1986**, *33*, 3628−3631.
(38) Murat, M.; Grest, G. S. *Macromolecules* **1996**, *29*, 1278−1285.

$$N_d = D(2^{G+1} - 1) \quad (5)$$

where G is the generation (the number of branch points between the core and terminal ends) and D is the number of bonds between branch points of functionality 3. Figure 2 provides schematic representations of the G2D1, G3D1, G2D2, and G0D15 architectures. We will present our results grouped by molecular weight to study the effect of branching at a constant molecular weight. This is achieved by increasing D as G decreases to zero, where G0 signifies a linear−linear block copolymer. An example of this are the architectures G3D1, G2D2, and G0D15 (shown in Figure 2), which have similar molecular weights near 45m.

The $A-A$ and $A-B$ interactions are purely repulsive and have a cutoff radii of $r_{cij} = 2^{1/6}\sigma$. The $B-B$ interactions have an attractive potential with a cutoff radii of $r_{cij} = 2.5\sigma$. One copolymer was arranged on a lattice grid, manually to ensure no chain crossing in the initial configuration, and then was replicated N_m times to achieve a specific number of molecules in a cubic box at the desired total concentration. The total copolymer concentration, $[X]$, is defined as $[X] = N_m N_b/V$ where N_m is the number of copolymer molecules, N_b is the number of monomer beads per copolymer molecule, and V is the total volume of the simulation space.

All simulations were run using periodic boundary conditions in all dimensions. All systems were run with at least $N_m = 125$ copolymer molecules. Many systems were tested with $N_m = 216$ or more and the most concentrated systems were run with $N_m = 1000$ to prevent the largest micelles from having a radius of gyration greater than one-fifth the box side. Size effects were determined to be present when simulations of the same concentration and architecture, but different numbers of molecules, showed different distributions of aggregate size or the radial distribution of aggregate center of mass. A system size of $N_m = 125$ copolymer molecules was found to be sufficient to obtain a CMC independent of the box size.

Copolymer molecules were designated as belonging to an aggregate if any linear tail monomers (type B) were within 1.5σ of each other, which is the distance at which the bond potential goes to infinity. The simulation temperature chosen was $k_B T/\epsilon[=]T^* = 1.8$. This was the lowest temperature at which all simulations maintained an equilibrium between aggregated and unaggregated molecules.

The simulations were carried out using LAMMPS,[39,40] with a time step of $\Delta t = 0.008\tau$. The system was run for 500 000 time steps with all cutoff radii set to $r_{cij} = 2^{1/6}\sigma$ to eliminate any bias from the initial configuration. The system was then allowed to equilibrate for 4 million time steps. The simulation was then run for at least 10 million time steps; for the more concentrated and slower relaxing systems 500 million time steps were needed. The length (time) of the simulation was evaluated by calculating the tracer autocorrelation function $C(t)$ defined as,

$$C(t) = \frac{\langle N(t_0 + t)\, N(t_0)\rangle - \langle N(t_0)\rangle^2}{\langle N^2(t_0)\rangle - \langle N(t_0)\rangle^2} \quad (6)$$

where $N(t)$ is the number of copolymers in the aggregate that a copolymer belongs to at time t and we average using every copolymer molecule as a tracer molecule and every time step as a time origin, t_0. The correlation time, τ_c, was the time required for $C(t) = e^{-1}$. Each simulation was run for at least $10\tau_c$ to have at least 10 independent configurations. Snapshots of the monomers' positions were saved every 10 000 or 100 000 time steps depending on the length of the simulation.

3. Results and Discussion

3.1. Critical Micelle Concentration. The CMC is one of the most commonly studied properties of a self-assembling system because it is a direct measure of the thermodynamic stability of the micelles in solution. To explore the effects of dendron generation and branching architecture on CMC for linear−dendritic block copolymers we simulated copolymers with a linear block length of 30 monomers and varied both dendron generation ($G = 2, 3, 4, 5$) and spacer length between branch points ($D = 1, 2, 4$). Figure 3 shows a plot of free copolymer concentration, $[X_1]$, against the total copolymer concentration, $[X]$ for copolymers with dendritic blocks of varying generation and spacer length of 1. The maximum free copolymer concentration for each curve defines the CMC for that system. In an ideal system one would expect the free copolymer concentration to plateau and remain constant at the CMC for total concentrations above the CMC. The maximum in free copolymer concentration versus total copolymer can be explained as follows. As more copolymer is added to the system, small aggregates begin to form, reducing the free copolymer concentration relative to the total copolymer concentration. After the CMC is reached, the free copolymer concentration drops as a result of excluded volume interactions between monomers that introduce nonideal behavior at high concentrations.[41] The CMC values for each simulated system are given in Table 1. Figure 4 summarizes the CMC data for each system simulated in this work by plotting CMC versus hydrophilic/hydrophobic molecular weight ratio. For comparison, the experimental CMC data from Nguyen and Hammond[5] for dendritic−linear−dendritic triblocks are also shown, which is different from the diblock architecture modeled in this study and this might exert an influence on the results. For a fixed spacer length, the CMC increases as the hydrophobic/hydrophilic molecular weight ratio decreases (i.e., the generation of the dendritic block increases). This trend qualitatively agrees with the experimental measurements from refs 5 and 10 (not shown). From Figure 4 it can be seen that the branching in the dendritic block results in a more dramatic increase in CMC at higher generations than one would expect for a linear−linear diblock copolymer with an equivalent total molecular weight and hydrophobic/hydrophilic molecular weight ratio. In the model systems, for a fixed molecular weight dendritic block, the CMC shifts to lower values as the number of spacer monomers (D) between branch points is increased. The increase in D increases the flexibility of the hydrophilic dendritic tail group, allowing it to pack more efficiently around the hydrophobic core. To date, we are unaware of any experimental reports that have explored the flexibility of the dendritic block on micellization properties by altering the chemical structure of the branches. The effect of dendron flexibility was studied in the experiments by Nguyen and Hammond by changing the pH of the solution. In their experimental system the dendritic block was a PAMAM dendron. At low pH, PAMAM is known to adopt an open, more rigid conformation due to electrostatic repulsions among the protonated amine groups along the branches. At high pH, PAMAM has a compact conformation because the amine groups are no longer protonated and the branches are more flexible.[42−44] Nguyen and Hammond observed that the CMC shifted to lower values as the pH was raised. Thus, it appears there is a connection between increased flexibility in the dendritic tail and lowering of the CMC, although additional simulations of the present model, with suitable parameter adjustments to capture the stiffening of the branches due to electrostatic repulsions are required to make a direct comparison to these experiments.

(39) Plimpton, S. *J. Comput. Phys.* **1995,** *117*, 1−19.
(40) http://lammps.sandia.gov/.
(41) von Gottberg, F. K.; Smith, K. A.; Hatton, T. A. *J. Chem. Phys.* **1997**, *106*, 9850−9857.
(42) Maiti, P. K.; Goddard, W. A. *J. Phys. Chem. B* **2006**, *110*, 25628−25632.
(43) Lee, H.; Baker, J. R.; Larson, R. G. *J. Phys. Chem. B* **2006**, *110*, 4014−4019.
(44) Optiz, A. W.; Wagner, N. J. *J. Polym. Sci., Part B* **2006**, *44*, 3026−3077.

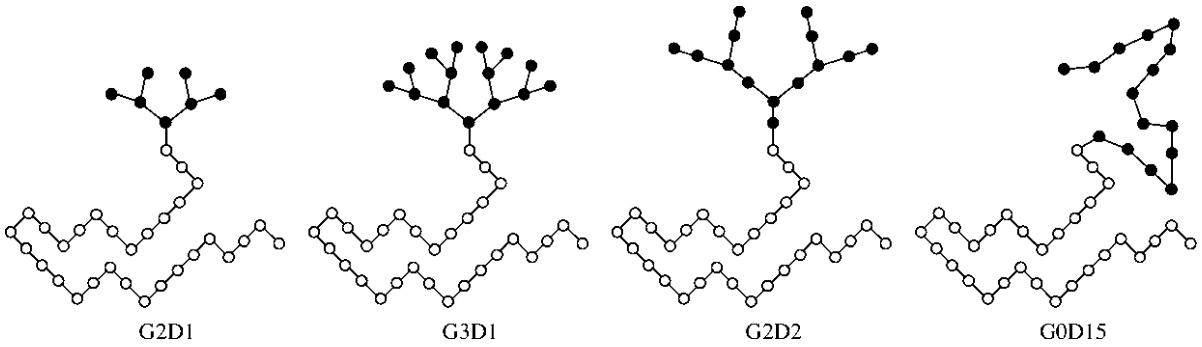

Figure 2. Model representation of the G2D1, G3D1, G2D2, and G0D15 architectures. The black circles represent hydrophilic monomers, and the open circles represent hydrophobic monomers.

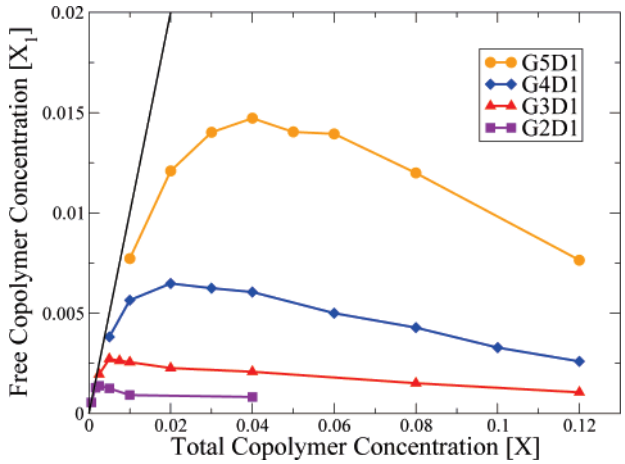

Figure 3. Concentration of free copolymers for different generations of the dendron block. The black line represents the ideal solution behavior of the copolymer solution, $[X_1] = [X]$. The lines are shown to guide the eye.

Table 1. CMC for Different Dendritic Architectures[a]

architecture	molecular weight	CMC	ratio	series
G2D1	37	0.0014	4.3	–
G3D1	45	0.0027	2.0	45
G2D2	44	0.0024	2.1	45
G0D15	45	0.0021	2.0	45
G4D1	61	0.0065	0.97	60
G3D2	60	0.0052	1.0	60
G2D4	58	0.0042	1.1	60
G0D31	61	0.0034	0.97	60
G5D1	93	0.0147	0.48	90
G4D2	92	0.0132	0.48	90
G3D4	90	0.0099	0.50	90
G2D9	93	0.0082	0.48	90
G0D63	93	0.0056	0.48	90

[a] Ratio refers to the ratio of the molecular weights of the hydrophobic block to the hydrophilic block. Vertical space separates groups with similar molecular weights.

3.2. Micelle Size and Shape. We now look at the effect of total concentration on the size distribution of aggregates. Figure 5 shows the distribution of G4D1 copolymers into aggregates. Free copolymer molecules are considered aggregates of 1 and thus the values at the origin are very large reflecting the relatively large number of unaggregated chains. We see that as the concentration increases, a Gaussian-shaped distribution forms with a mean that increases with concentration. We note that the CMC for G4D1 was observed in Figure 3 at [X] = 0.02 and it is at this concentration where we begin to see large clusters forming.

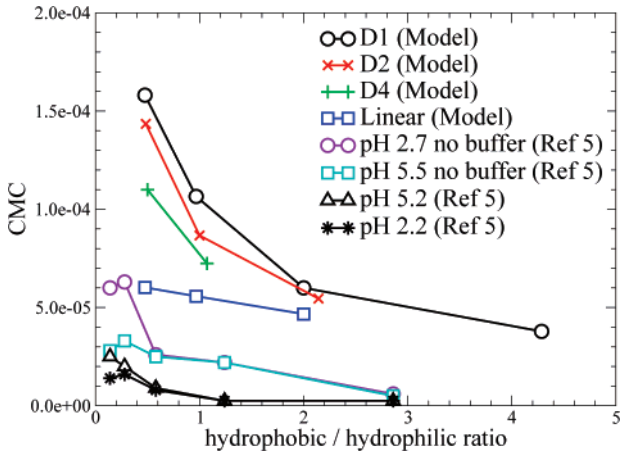

Figure 4. CMC versus hydrophilic/hydrophobic ratio for the model system (D1, D2, D4, linear) and experimental results from ref 5. The units of CMC are in M for the experimental data and molecules/unit volume for the simulation data. The generation (G) of each point can be determined by comparing the spacer length (D) and ratio in Table 1. Lines are drawn between points to guide the eye.

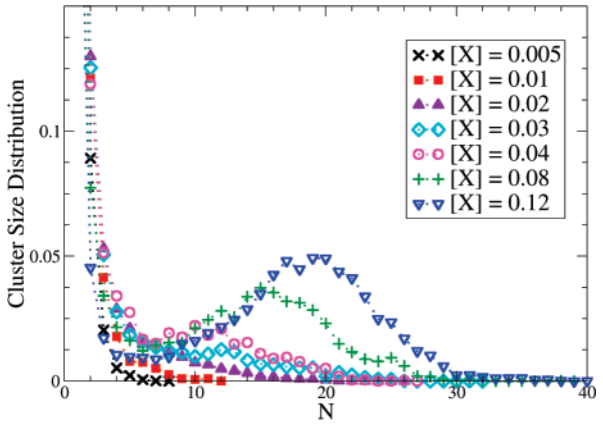

Figure 5. Cluster size distributions for the G4D1 architecture at different total concentrations. The lines are shown to guide the eye.

We now focus on the most concentrated systems ($[X] = 0.12$) to look at the structure of the aggregates, as that is where the most aggregates are found. Figure 6 shows the distribution of copolymers into aggregates for the most concentrated system. We see that the most probable number of copolymer molecules per aggregate increases as we decrease the generation of the dendritic block. Figure 7 shows snapshots of an aggregate for the G0D15, G3D1, and G5D1 architectures for the most probable number of molecules. The density profile for the aggregates with the most probable number of molecules (as determined in Figure 6) is shown in Figure 8. We see by comparing G3D1, G4D1, and G5D1 on (a), (b), and (c) of Figure 8 that increasing the molecular

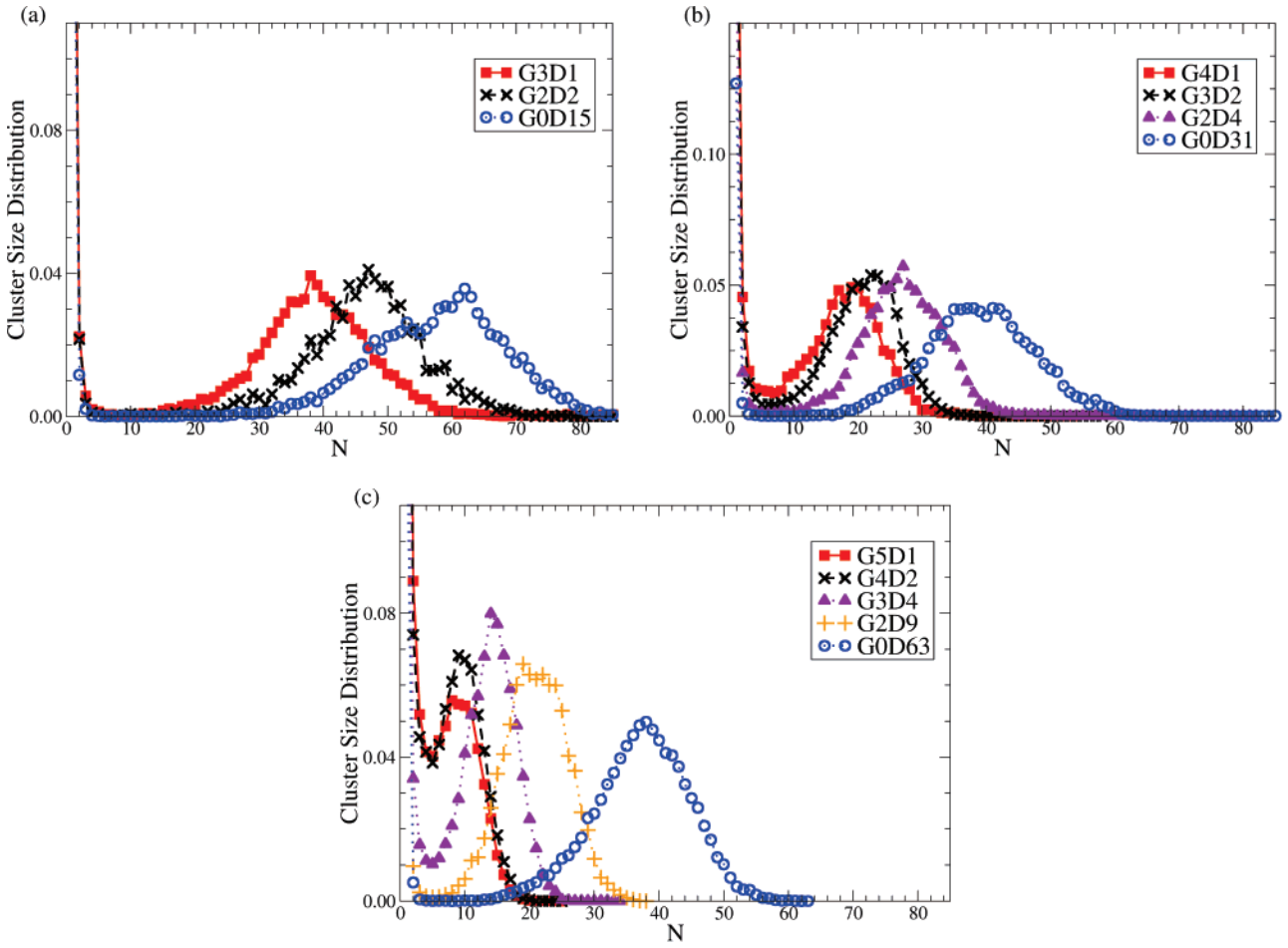

Figure 6. Cluster size distribution at $[X] = 0.12$ for the different architectures at similar molecular weights: (a) 45*m*, (b) 61*m*, and (c) 93*m*. *N* is the number of copolymers per aggregate. The lines are shown to guide the eye.

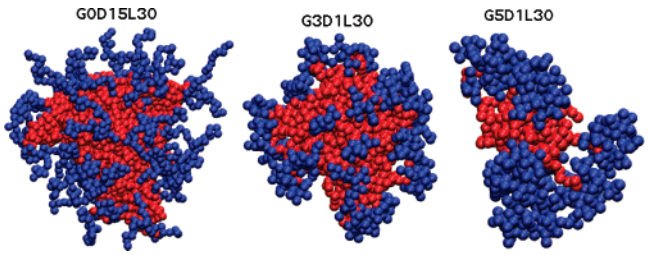

Figure 7. Snapshots of micelles of the G0D15L30, G3D1L30, and G5D1L30 systems at the most probable micelle number as determined in Figure 6 and listed in Table 2. The hydrophobic and hydrophilic monomers are shown as red and blue, respectively. Each snapshot is shown at a different scale.

weight of the dendritic block decreases the size of the hydrophobic core. This observation agrees with experimental results.[5] We also see that when the dendrimer generation is increased, while keeping the molecular weight constant, the size of the core decreases while increasing the density of hydrophilic monomers at the surface of the core. This shows that the architecture of the dendritic block can be used to control the size of the micelle.

It is also desirable to know if we can control the shape of micelles, as it was shown experimentally[3] with a block copolymer of hydrophilic poly(propylene imine) dendron and polystyrene that the aggregate changed from inverted micelles to spherical vesicles to rod shaped micelles to spherical micelles as the generation increased from 2 to 5 in a mixture of toluene and water. Table 2 shows the characteristic size and shape of the most probable (N_{mode}) aggregate for each architecture variant.

We describe the shape of the aggregates by calculating the asphericity,[45,46]

$$\delta = 1 - 3\frac{\langle I_2 \rangle}{\langle I_1^2 \rangle} \tag{7}$$

where I_1 and I_2 are the first two invariants,

$$I_1 = \lambda_1 + \lambda_2 + \lambda_3 \tag{8}$$

$$I_2 = \lambda_1\lambda_2 + \lambda_2\lambda_3 + \lambda_1\lambda_3 \tag{9}$$

λ_i is an eigenvalue of the gyration tensor,

$$G_{uv} = \frac{1}{N}\sum_i^N (r_{ui} - R_u)(r_{vi} - R_v) \tag{10}$$

where R is the center of mass and u and $v = x$, y, and z. The asphericity parameter can take values ranging from 0 (sphere) to 1 (line). The standard deviation, σ_q, of a quantity q presented in Table 2 is calculated using the expression:[33]

$$\sigma_q = \sqrt{\frac{2\tau_c}{t_{max}}(\overline{q^2} - \overline{q}^2)} \tag{11}$$

(45) Rudnick, J.; Gaspari, G. *J. Phys. A* **1986**, *19*, L191−L193.
(46) Aronovitz, J.; Nelson, D. *J. Phys.* **1986**, *47*, 1445−1456.

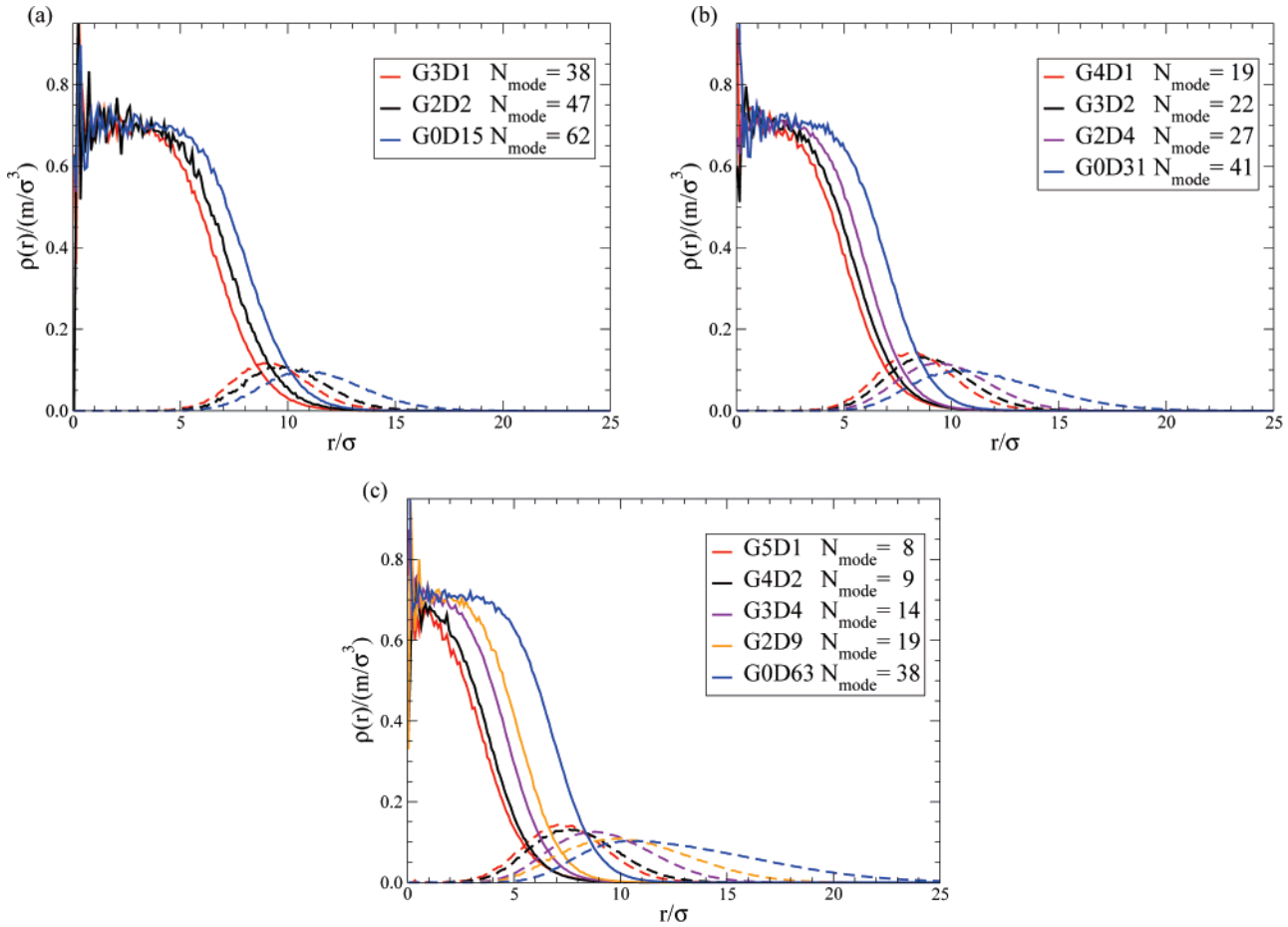

Figure 8. Density profile of aggregates of N_{mode} copolymers at $[X] = 0.12$ for the different architectures at similar molecular weights: (a) 45*m*, (b) 61*m*, and (c) 93*m*. The solid and dashed lines are the density profile of hydrophobic and hydrophilic monomers, respectively.

Table 2. Characteristics of Most Probable Aggregates[a]

arch.	N_{mode}	$\langle R_g^2 \rangle$	$\langle \delta \rangle$	$\langle R_g^2 \rangle_{core}$	$\langle \delta \rangle_{core}$	$\langle R_g^2 \rangle_{free}$
G3D1	38	62.2 (0.4)	0.038 (0.003)	41.9 (0.4)	0.065 (0.006)	9.0 (0.4)
G2D2	47	69.4 (0.8)	0.038 (0.007)	46.9 (0.8)	0.071 (0.011)	9.6 (0.9)
G0D15	62	87.9 (1.0)	0.029 (0.007)	54.2 (1.0)	0.064 (0.014)	11.9 (1.2)
G4D1	19	59.5 (1.1)	0.042 (0.008)	30.1 (1.0)	0.083 (0.016)	10.7 (0.8)
G3D2	22	65.4 (1.2)	0.036 (0.007)	31.1 (1.0)	0.081 (0.017)	11.8 (0.9)
G2D4	27	73.5 (1.5)	0.028 (0.008)	33.4 (1.3)	0.069 (0.019)	13.7 (1.5)
G0D31	41	111.8 (1.7)	0.017 (0.005)	41.5 (1.1)	0.057 (0.018)	20.1 (3.1)
G5D1	8	56.9 (1.4)	0.071 (0.010)	21.4 (1.0)	0.12 (0.019)	12.2 (0.6)
G4D2	9	62.8 (1.6)	0.052 (0.010)	20.7 (1.0)	0.11 (0.023)	14.9 (0.8)
G3D4	14	83.0 (1.1)	0.032 (0.005)	23.9 (0.7)	0.086 (0.014)	18.8 (0.9)
G2D9	19	112.6 (2.4)	0.023 (0.006)	27.2 (1.0)	0.072 (0.022)	24.8 (2.7)
G0D63	38	191.4 (2.2)	0.015 (0.003)	39.7 (0.7)	0.051 (0.011)	37.2 (6.6)

[a] One standard deviation is inside the parentheses. The subscript 'core' refers to the property for the hydrophobic core. The subscript 'free' refers to the property of a free copolymer molecule. Vertical space separates groups with similar molecular weights.

where τ_c is the correlation time defined in the Method section, $\bar{q}$ is the average value of q, and t_{max} is the total time of the simulation.

We see that the aggregates become less spherical as the generation of the dendritic block increases; this is even more apparent when we consider the shape of the core. We also see evidence that the corona shrinks as the generation increases in Table 2 when we look at the ratio of the radii of gyrations for the micelle to the core.

4. Conclusions

In this study, we simulated linear−dendritic diblock copolymers in a solution that favors the dendritic block to investigate the effects of dendron molecular weight and architecture on micelle properties. The simulation results obtained with a simple, coarse-grained model agree qualitatively with available experimental data. Specifically, we find that the CMC increases with dendron generation for a fixed dendritic architecture. This increase is shown to be higher than what would be expected for a traditional linear diblock copolymer.

Upon comparing block copolymer systems with the same total molecular weight and hydrophilic-to-hydrophobic ratio, we find that the CMC decreases as the number of spacer monomers between branch points in the dendron increases. The increase in spacer monomers increases the flexibility of the dendritic block and promotes better packing of the hydrophilic monomers around

the hydrophobic core. The same trend is seen in experiments on linear−dendritic block copolymers when pH is raised, effectively increasing the flexibility of the dendritic block.

In agreement with reported experiments, the size of the micelle decreases as the generation (i.e., molecular weight) of the dendritic block increases. Cluster size distributions for block copolymers of similar total molecular weights show that micelle size can be controlled by carefully selecting dendritic architecture. The use of dendritic blocks focuses the hydrophilic corona into a higher-density region around the core compared to traditional linear diblock copolymers. This high-density corona promotes the presentation of many dendron "ends" at the surface of the micelle that could be functionalized with targeting ligands for applications in drug delivery and sensing.

The goal of this study was to examine the influence of dendron properties on micellization, and thus, the linear polymer block length and interactions were held fixed. A complementary investigation of how altering the molecular weight and interactions of the linear polymer block attached to a dendron of fixed molecular weight and architecture impact micellar problems should provide additional useful insight about this interesting class of copolymer.

Acknowledgment. The computations were performed in part at the ISU High Performance Computing facility. We are grateful to P. T. Hammond for helpful discussions.

LA703006W